A non-NH$_3$ pathway for NO$_x$ conversion in coupled LNT-SCR systems

Jin Wang [a], Yaying Ji [a], Zhengwang He [a], Mark Crocker [a,*], Mark Dearth [b], Robert W. McCabe [b]

[a] Center for Applied Energy Research, University of Kentucky, Lexington, KY 40511, USA
[b] Chemical Engineering Department, Ford Motor Co., Dearborn, MI 48124, USA

ARTICLE INFO

ABSTRACT

NO$_x$ storage-reduction experiments were performed using a coupled LNT-SCR system consisting of a low-precious metal loaded Pt/Rh LNT catalyst and a commercial Cu–zeolite SCR catalyst. Cycling experiments revealed that when a CO + H$_2$ + C$_3$H$_6$ mixture or C$_3$H$_6$ by itself was used as the reductant, the NO$_x$ conversion over the SCR catalyst exceeded the conversion of NH$_3$ over the same catalyst. This is explained by the presence of propene, which slipped through the LNT catalyst and reacted with the LNT NO$_x$ slip. Separate experiments, conducted under continuous flow and lean-rich cycling conditions, confirmed the ability of propene, as well as ethene, to function as a NO$_x$ reductant over the SCR catalyst. Cycling experiments also revealed that the SCR catalyst was able to store propene, such that NO$_x$ reduction by stored propene continued into the lean phase (after the switch from rich conditions). According to adsorption experiments, significant co-adsorption of NH$_3$ and propene occured in the SCR catalyst, while under lean-rich cycling conditions the contributions of NH$_3$ and C$_3$H$_6$ to NO$_x$ conversion were found to be essentially additive. These findings suggest that under actual driving conditions, NO$_x$ reduction by non-NH$_3$ reductants (olefins and possibly other hydrocarbons) in the SCR catalyst can contribute to the mitigation of lean and rich phase NO$_x$.

1. Introduction

Lean-burn engines provide more efficient fuel combustion and lower CO$_2$ emissions compared with traditional stoichiometric engines. However, the effective removal of NO$_x$ from lean exhaust represents a challenge to the automotive industry. In this context, Lean NO$_x$ Trap (LNT) catalysts represent a promising technology, particularly for light duty diesel and gasoline lean-burn applications. Moreover, recent studies have shown that the performance of LNTs can be significantly improved by adding an in situ selective catalytic reduction (SCR) catalyst in series downstream [1–18]. In this configuration the SCR catalyst functions in a passive or in situ mode, i.e., with the storage and utilization of NH$_3$ generated by the LNT during rich purge events.

In comparison with competing NO$_x$ reduction technologies such as urea SCR, the LNT-SCR system has several significant benefits. Most importantly, the LNT-SCR system requires only fuel as the reductant and therefore eliminates the need and associated costs for urea injection into the exhaust gas. The LNT-SCR system also has several advantages over an LNT-only system. The SCR catalyst eliminates NH$_3$ slip from the LNT by storing it and subsequently catalyzing its reaction with unreacted NO$_x$ from the LNT. The benefit

is greatest at low temperatures (<300 °C), given that LNT catalysts typically display the highest NH$_3$ selectivity and the lowest NO$_x$ conversion in this temperature region [19,20]. As a result of the additional reduction in undesirable NH$_3$ slip, lean-phase NO$_x$ breakthrough, and rich-phase NO$_x$ spikes, significantly improved NO$_x$ conversion (i.e., NO$_x$ to N$_2$) can be realized by the coupled system. The LNT-SCR system can also provide improved performance at high temperatures. Nitrates formed in the LNT at high temperatures are less stable than at lower temperatures, resulting in high NO$_x$ spikes at the lean/rich transition which lower the overall NO$_x$ conversion. The NH$_3$-SCR component dampens this portion of released NO$_x$ by facilitating reaction of the NO$_x$ with stored NH$_3$. To extend the benefits of the LNT-SCR synergy to these higher temperatures, it has been suggested that the SCR catalyst should ideally be operated at somewhat lower temperatures than the LNT in order to achieve better NH$_3$ adsorption capacity [15,21], although this may not be desirable for systems in which the LNT already operates at a marginally low temperature.

Given that the presence of the SCR catalyst relaxes the NO$_x$ conversion requirements of the LNT catalyst, the volume of the LNT in the LNT-SCR system can, in principle, be lower than for an LNT-only system, thereby reducing the precious metal costs for the system [14]. Moreover, recent work suggests that the LNT-SCR concept can afford additional benefits. Xu et al. [14] have reported that H$_2$S emissions during LNT desulfation are lowered when an SCR catalyst is present, due to the ability of the SCR catalyst to catalyze the

oxidation of H_2S with residual oxygen on the catalyst. Furthermore, Seo et al. [22] report significant improvements in $deNO_x$ performance and the reduction of NH_3 slip for hydrothermally aged LNT catalysts over which more NH_3 was generated than for their fresh analogs. In such aged systems, the SCR catalyst effectively compensates for the lost activity of the LNT by converting NO_x that slips through the LNT [14,22]. Chatterjee et al. [15] demonstrated the synergy of LNT and SCR catalysts in a combined system through simulations, and confirmed that the positive effect of the downstream SCR catalyst became more important in the case of an aged LNT which typically produces more NH_3.

We have previously reported laboratory reactor experiments on a proto-typical LNT-SCR system and have performed initial vehicle tests which confirm the promise of this approach [11,14]. During mechanistic investigations we have observed that in addition to the NH_3 pathway for NO_x conversion, a second pathway can operate in the SCR catalyst of LNT-SCR systems which is associated with the presence of hydrocarbons [14]. It should be appreciated that during engine-based LNT regeneration, significant amounts of hydrocarbons can be present in the rich gas produced by the engine. Indeed, depending on the regeneration strategy adopted, peak hydrocarbon concentrations approach 10,000 ppm (expressed as C1 equivalents), corresponding mainly to lower hydrocarbons such as methane, ethene, ethane, propene, etc. [23]. In this paper we present our efforts to characterize this second NO_x conversion pathway.

2. Experimental

2.1. Catalysts

Two catalysts were used in this study, comprising a low-precious metal loaded Pt/Rh LNT catalyst and a commercial SCR catalyst of the Cu–zeolite type. The LNT catalyst contained BaO as the main NO_x storage material, as well as a ceria-based oxygen storage material, and Pt and Rh as the precious metals. Both catalysts were provided by BASF and were prepared on 400 cpsi/6.5 mil ceramic monoliths. For bench reactor tests, 7.5 cm (l) × 2.1 cm (d) core samples of each catalyst were drilled from the monoliths.

2.2. LNT-SCR lean-rich cycling experiments

Catalyst tests were performed on a synthetic gas bench reactor. The LNT and SCR monolith cores were wrapped in Zetex insulation tape and inserted into separate vertical reactor tubes (2.2 cm inner diameter) which were independently heated by two electric furnaces. The catalysts were positioned in series, the inlet face of the SCR catalyst monolith being 10″ downstream of the outlet face of the LNT monolith. A gas sampling port was positioned between the catalysts to enable analysis of the effluent gas from the LNT catalyst. Simulated exhaust gas mixtures were introduced to the LNT

reactor from pressurized gas bottles. Water was introduced by a peristaltic cartridge pump (Cole–Parmer) to a heated zone, vaporized and added to the simulated exhaust mixture. A rapid switching 4-way valve system was used to alternate between the lean and rich gas mixtures so that the lean/rich/lean transitions in these experiments were almost instantaneous (within 0.2 s). K-type thermocouples were placed at the LNT inlet, mid-point and exit, and the SCR catalyst inlet and outlet, to monitor the temperature profiles. A multi-gas analyzer (MKS Model 2030) was used to monitor the concentrations of NO, NO_2, N_2O, NH_3, CO, CO_2, H_2O both between the LNT and SCR catalysts and at the outlet of the SCR catalyst. During lean-rich cycling, the observed catalyst breakthrough profiles stabilized to a fixed limit cycle in about 2 h, at which point it was possible to characterize the performance in terms of the 'stationary' concentration cycles. Data were collected in the range of 150–450 °C, using a temperature ramp of 10 °C/min between measurement points. Once at the measurement temperature, the reactor was monitored until no changes in effluent composition were observed from one cycle to the next (about 2 h, as indicated above), at which point data were collected. The conditions for the cycling experiments are summarized in Table 1. The selectivity to N_2 during rich purges was determined by difference (i.e., $S_{N_2} = 100\% - S_{N_2O} - S_{NH_3}$). Before beginning the measurements, catalysts were de-greened by exposing them to lean-rich cycling conditions at 500 °C for 5 h, using the lean gas feed and the rich gas mixture #1 shown in Table 1.

2.3. NO_x reduction experiments over SCR catalyst under continuous flow and lean-rich cycling conditions

Experiments were performed in the synthetic gas bench reactor described above using a 7.5 cm (l) × 2.1 cm (d) monolith sample of the SCR catalyst. The total feed gas flow rate was set to 13,719 sccm, giving a GHSV of 30,000 h^{-1}. Two K-type thermocouples were placed just before the SCR catalyst and at the catalyst outlet to monitor the temperature profile. A multi-gas analyzer (MKS Model 2030) was used to monitor the concentrations of NO, NO_2, N_2O, NH_3, C_3H_6, C_2H_4, CO, CO_2 and H_2O in the feed and reactor effluent. Before beginning each series of measurements, the catalyst was pre-treated in a flowing mixture of 8% O_2, 5% CO_2, 5% H_2O and N_2 (balance) at 500 °C for 3 h.

For the continuous flow experiments, the catalyst was heated to 200 °C under a flowing feed of 5% CO_2, 5% H_2O and N_2 (balance), after which NO (300 ppm), O_2 (as indicated) and the reductant (3333 ppm C_3H_6 or 5000 ppm C_2H_4) was added to the feed. NO_x reduction measurements were performed under steady state conditions at intervals of 25 °C in the temperature range of 200–550 °C.

For the lean-rich cycling experiments, the catalyst was similarly heated to 200 °C under a flowing feed of 5% CO_2, 5% H_2O and N_2 (balance), after which cycling was commenced. The feed gas composition used was: lean (60 s): 300 ppm NO, 8% O_2, 5% CO_2, 5% H_2O, N_2 as balance; rich (5 s): 300 ppm NO, 3333 ppm C_3H_6 or

Table 1

Base conditions used for NO_x storage-reduction cycling experiments. Note that the same lean phase conditions (as shown) were used for all experiments.

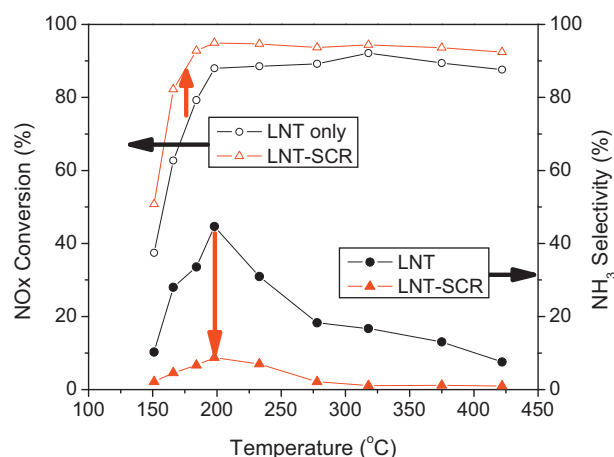| Parameter	Lean	Rich #1	Rich #2	Rich #3	Rich #4	Rich #5
Duration (s)	60	5	5	5	5	5
Temperature (°C)	150–450	150–450	150–450	150–450	150–450	150–450
Space velocity (h^{-1})	30,000	30,000	30,000	30,000	30,000	30,000
NO (ppm)	300	300	300	300	300	300
O_2 (%)	8	1	1	1	1	1
CO (%)	–	4	1	1	–	–
H_2 (%)	–	1.3	0.33	0.33	–	–
C_2H_4 (ppm)	–	–	–	5000	–	5000
C_3H_6 (ppm)	–	–	3333	–	3333	–
CO_2 (%)	5	5	5	5	5	5
H_2O (%)	5	5	5	5	5	5
N_2 (%)	Balance	Balance	Balance	Balance	Balance	Balance

Fig. 1. Comparison of cycle-averaged NO_x conversion and selectivity to NH_3 for LNT-only and LNT-SCR systems using 4% CO + 1.3% H_2 as reductant.

Fig. 2. Comparison of cycle-averaged NO_x conversion and selectivity to NH_3 for LNT-only and LNT-SCR systems using 1% CO + 0.33% H_2 + 3333 ppm C_3H_6 as reductant.

5000 ppm C_2H_4, 0% or 1% O_2 (as indicated), 5% CO_2, 5% H_2O, N_2 as balance. Measurements were recorded once 'stationary' concentration cycles were attained. Data were recorded at intervals of 25 °C in the temperature range of 150–450 °C.

2.4. C_3H_6 and NH_3 adsorption experiments

Adsorption experiments were performed using the same sized catalyst sample and the same reactor described in the preceding section. Before each experiment, the catalyst was pretreated by exposing it to a flow containing 8% O_2, 5% CO_2, 5% H_2O and N_2 (balance) at 600 °C for 2 h, followed by cooling to the desired temperature in the flowing gas. The feed was then switched to one containing 500 ppm adsorbate (C_3H_6 or NH_3, with 5% CO_2, 5% H_2O and N_2 as balance also present), until the catalyst reached saturation. In co-adsorption experiments, 500 ppm C_3H_6 and 500 ppm NH_3 were added to the reactor feed. Next, the sample was flushed with 5% CO_2, 5% H_2O and N_2 to remove weakly adsorbed reductant until it was no longer detected in the reactor effluent. For the experiments involving NH_3, the reactor was run in bypass mode for 1 h before the adsorption measurements in order to saturate the surface of the gas lines running to the gas analyzer with NH_3. The adsorption capacity of the catalyst was calculated from the uptake profile, with subtraction of the amount of adsorbate released during flushing.

3. Results and discussion

3.1. LNT-SCR system behavior under lean-rich cycling

In order to investigate LNT-SCR system performance with different NO_x reductants, lean-rich cycling experiments were performed using different feed gas compositions in the rich phase (see Table 1). Fig. 1 shows a comparison of the cycle-averaged NO_x conversions obtained for the LNT-SCR system and a LNT-only system when using a mixture of 4% CO and 1.3% H_2 as the rich phase reductant (rich phase condition #1 in Table 1). Note that each set of LNT-only and LNT-SCR results correspond to one experiment, i.e., the LNT-only results are based on the gas composition measured between the LNT and SCR catalysts. As shown, the LNT-SCR system affords slightly higher NO_x conversion levels across the entire temperature window examined (150–450 °C). Simultaneously, a decrease is observed in NH_3 emissions from the LNT-SCR system as compared to the LNT-only configuration. This is reflected in the decreased overall system selectivity to NH_3, which is also depicted in Fig. 1. The corresponding nitrogen balance over the SCR catalyst
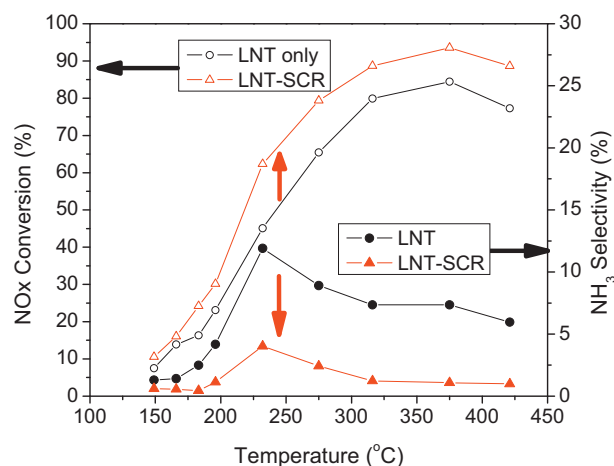
(data not shown) reveals that in no case does the amount of NO_x converted (in μmol) across the SCR catalyst exceed the amount of NH_3 removed, which is consistent with NO_x conversion occurring via selective catalytic reduction with NH_3. Indeed, in general the amount of NH_3 converted slightly exceeds that of NO_x converted, suggesting that excess NH_3 can undergo oxidation by O_2 on the catalyst, which in keeping with other Cu–zeolite catalysts would be expected to yield mainly N_2 [24,25]. Additionally, it is possible that the NO_x:NH_3 reaction stoichiometry is not exactly 1:1. However, a significant deviation from 1:1 stoichiometry is unlikely given that the NO_2:NO ratio of NO_x entering the SCR catalyst typically did not exceed 1:1 during cycling, i.e., NO_x conversion should proceed according to the 1:1 NO_x:NH_3 stoichiometry depicted in Eqs. (1) and (2).

$$4NO + 4NH_3 + O_2 \rightarrow 4N_2 + 6H_2O \tag{1}$$

$$NO + NO_2 + 2NH_3 \rightarrow 2N_2 + 3H_2O \tag{2}$$
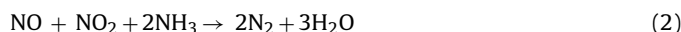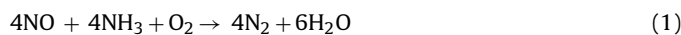
The foregoing results are consistent with a model in which rich phase NH_3 slip from the LNT catalyst is stored on the SCR catalyst and subsequently undergoes reaction with lean phase NO_x slip from the LNT.

In order to examine the consequences of hydrocarbon addition, cycling experiments were conducted in which 1% CO + 0.33% H_2 + 3333 ppm C_3H_6 and 1% CO + 0.33% H_2 + 5000 ppm C_2H_4 were used as the rich phase reductant mixtures (corresponding to respectively rich phase conditions #2 and 3 in Table 1). The low CO and H_2 concentrations of respectively 1.0 and 0.33% were used to limit the overall NO_x conversion, as well as the amount of NH_3 emitted by the LNT, thereby ensuring that NH_3 slip from the LNT was not in excess relative to slipped NO_x. In this manner, differences in system performance could be readily detected. Fig. 2 compares NO_x conversion as a function of temperature for the LNT-SCR and LNT-only systems when using 1% CO + 0.33% H_2 + 3333 ppm C_3H_6 as the reductant mix. The low temperature performance of the LNT-SCR and LNT-only systems is particularly affected by the low reductant concentration, since LNT catalysts are unable to use reductants efficiently at low temperature (<250 °C). This is a consequence of the slow kinetics of NO_x reduction in this temperature region, together with the fact that the water–gas shift reaction for H_2 generation, which is the most active NO_x reductant at low temperature [26,27], is also typically kinetically limited in this temperature window [28]. Hence, with only a slight excess of reductant, and more particularly H_2, NO_x conversion is poor at low temperature.

As shown in Fig. 2, when using the 1% CO + 0.33% H_2 + 3333 ppm C_3H_6 reductant mixture the presence of the SCR catalyst is again
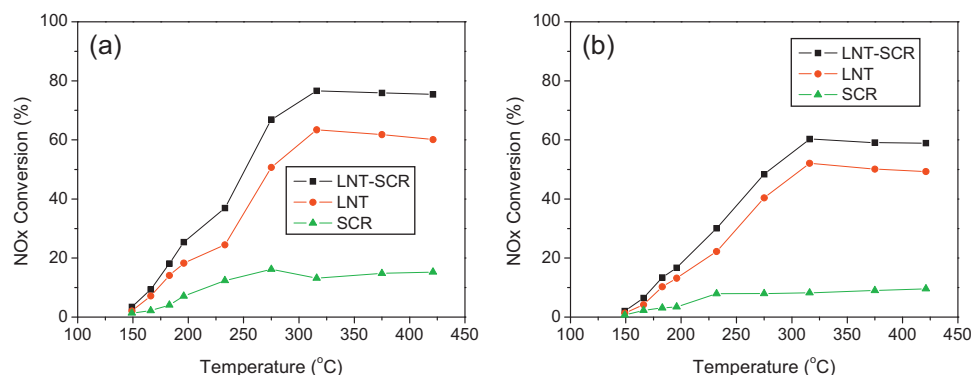
Fig. 3. NO_x conversion over LNT and SCR catalysts in LNT-SCR system during lean-rich cycling: (a) 3333 ppm C_3H_6 as reductant; (b) 5000 ppm C_2H_4 as reductant.

beneficial with respect to NO_x conversion. Indeed, appreciable NO_x conversion is observed over the SCR catalyst at temperatures in excess of 200 °C as indicated by the difference between the NO_x conversion measured for the LNT-only and LNT-SCR systems. Concomitantly, NH_3 emitted by the LNT is largely consumed by the SCR catalyst, although the selectivity to NH_3 shown by the LNT catalyst is low. Nitrogen balances for the LNT-SCR system using the 1% $CO + 0.33\%$ $H_2 + 3333$ ppm C_3H_6 and 1% $CO + 0.33\%$ $H_2 + 5000$ ppm C_2H_4 feeds are shown in Tables 2 and 3, respectively. Notably, for the feed containing C_3H_6, the amount of NO_x converted over the SCR catalyst exceeds the amount of NH_3 converted at all temperatures. Similarly, for the C_2H_4-containing feed the amount of NO_x converted exceeds the NH_3 converted, albeit that the differences between the two values are less pronounced than for the propene case. These experiments were performed multiple times and the results found to be repeatable; hence they are believed to be valid, as opposed to being an artifact caused by the system not being at (cycle-averaged) steady state. These results suggest that together with NH_3, a second reductant is present that can participate in NO_x reduction in the SCR catalyst. In order to ascertain whether the olefin, or a derivative thereof, also participates in NO_x reduction over the SCR catalyst, cycling experiments were performed in which 3333 ppm propene or 5000 ppm ethene was used as the only

reductant. Table 4 collects the results of these experiments and shows a breakdown of the cycle-averaged NO_x conversion measured at 233 °C across the LNT and SCR catalysts. For comparison purposes, data are included for the experiments in which CO and H_2 were also included in the feed with the olefin. As shown, NO_x conversion was observed across the SCR catalyst, even when using 3333 ppm C_3H_6 or 5000 ppm C_2H_4 as the sole reductant. Fig. 3 provides additional detail, showing the NO_x conversion across the LNT and SCR as a function of temperature for the experiments using C_3H_6 and C_2H_4 as the reductant. In both cases NO_x conversion is significant above 200 °C, reaching a maximum of 14% across the SCR catalyst at 421 °C when propene is used as the reductant. Indeed, propene affords higher levels of NO_x conversion than ethene over both the LNT and SCR catalyst, reflecting its superior activity as a NO_x reductant. Overall, these results clearly show that the olefin, or a derivative thereof, can participate in NO_x reduction over the SCR catalyst.

Fig. 4 compares the NO_x concentration profiles during cycling for the LNT-only and LNT-SCR systems using 1% $CO + 0.33\%$ $H_2 + 3333$ ppm C_3H_6, 3333 ppm C_3H_6 and 5000 ppm C_2H_4 as the rich phase reductants. In each case, the peak rich phase NO_x release (the so-called NO_x puff) is clearly decreased in the effluent gas from the SCR catalyst relative to the LNT effluent, while the lean phase NO_x slip is almost the same. These results suggest that propene, or a propene-derived product, can react with NO_x in the rich phase to afford NO_x reduction products. Also shown are the measured olefin and NH_3 concentrations in the LNT and SCR catalyst effluents during the cycling experiments. These profiles highlight the fact that a small amount of NH_3 is produced by the LNT, nearly all of which is converted over the SCR catalyst. However, in each case the amount of NO_x converted over the SCR catalyst consistently exceeds the NH_3 converted. For example, for the run using 3333 ppm C_3H_6, at 233 °C the amount of NO_x converted (22.7 μmol) greatly exceeds the NH_3 converted (1.2 μmol), while the C_3H_6 conversion across the SCR catalyst amounts to 261 μmol. Due to the comparatively long measurement time of the FTIR instrument used for the gas analyses (relative to the duration of the rich phase), it is not possible to give an exact breakdown with respect to the lean and rich phase NO_x

Table 2
Comparison of NO_x and NH_3 conversion over SCR catalyst in LNT-SCR system: rich condition #2 (propene as hydrocarbon).

Temperature (°C)	NH_3 converted across SCR (μmol)	NO_x converted across SCR (μmol)	NH_3 converted – NO_x converted (μmol)
183	0.6	14.6	−14.1
196	1.2	13.2	−12.0
233	5.3	32.2	−26.9
275	7.3	26.0	−18.7
316	8.9	16.4	−7.5
375	9.7	17.0	−7.2
421	7.0	21.2	−14.3

Table 3
Comparison of NO_x and NH_3 conversion over SCR catalyst in LNT-SCR system: rich condition #3 (ethene as hydrocarbon).

Temperature (°C)	NH_3 converted across SCR (μmol)	NO_x converted across SCR (μmol)	NH_3 converted – NO_x converted (μmol)
182	1.5	5.6	−4.1
197	2.1	5.8	−3.7
234	3.5	16.7	−13.2
276	7.6	13.5	−5.9
317	7.9	13.4	−5.5
376	4.8	11.4	−6.6
421	2.7	12.5	−7.8

Table 4
NO_x conversion over LNT and SCR catalysts in LNT-SCR system during lean-rich cycling measured at 233 °C for different reductants.[a]

Reductant	NO_x conversion (%)		
	LNT–SCR	LNT	SCR
$CO/H_2/C_2H_4$	38.7	29.6	9.1
$CO/H_2/C_3H_6$	62.3	45.1	17.3
C_2H_4	30.0	24.8	5.3
C_3H_6	36.9	24.6	12.3

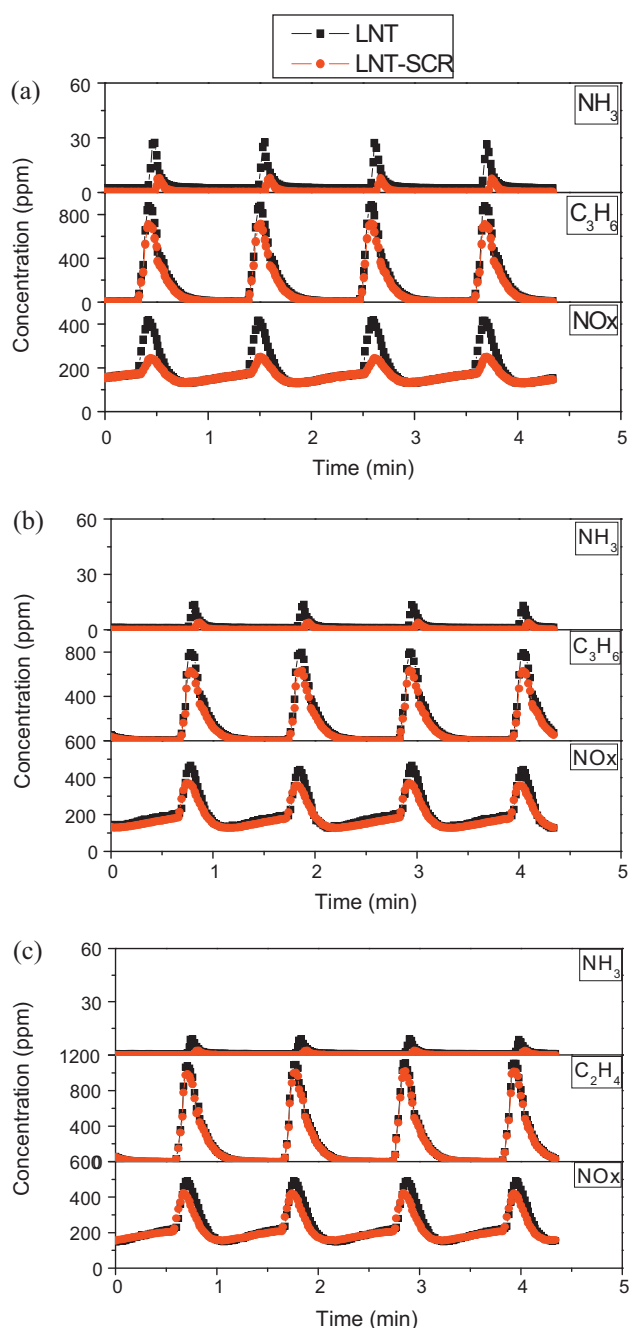[a] Reductant concentrations: 1% CO, 0.33% H_2, 5000 ppm C_2H_4, 3333 ppm C_3H_6.

Fig. 4. Comparison of gas composition behind LNT and SCR catalysts during lean-rich cycling at 233 °C using (a) 1% CO + 0.33% H_2 + 3333 ppm C_3H_6, (b) 3333 ppm C_3H_6 and (c) 5000 ppm C_2H_4 as reductant.

conversion over the SCR catalyst. However, a rudimentary analysis of the shape of the NO_x profiles suggests that significant NO_x conversion over the SCR catalyst occurs in the rich phase, although NO_x conversion may also occur during the rich to lean transition and its immediate aftermath. This is discussed more fully in section 3.3 below.

In an effort to ascertain whether propene-derived species were being formed over the LNT catalyst in the above experiments (which might function as NO_x reductants over the SCR catalyst), the effluent gas from the LNT was analyzed using an FT-IR gas analyzer. No significant formation of oxygenated species such as acrolein, acetaldehyde, isocyanic acid, etc., was observed (detection limit ca. 10 ppm), nor any other species that might function as a NO_x reductant. Small amounts of HCN were observed when
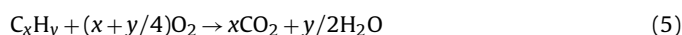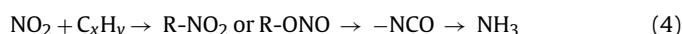
using 1% CO + 0.33% H_2 as the reductant (peak rich phase HCN concentration of 20 ppm), however, HCN formation decreased upon addition of 3333 ppm C_3H_6 to the reductant mix (peak HCN concentration of ~10 ppm), and HCN formation was not observed when only 3333 ppm C_3H_6 was used as the reductant. These findings therefore indicate that propene itself functioned as the primary NO_x reductant.

Finally, it should be mentioned that N_2O formation was observed in these experiments at temperatures of around 200 °C and lower. For example, using 1% CO + 0.33% H_2 + 3333 ppm C_3H_6 in the rich phase, 42% selectivity to N_2O was measured over the LNT catalyst at 196 °C, which dropped to <2% at 275 °C. However, for this reductant mix, it was found that a net conversion of N_2O occurred over the downstream SCR catalyst (up to 50%), presumably due to the reduction of N_2O by C_3H_6. This phenomenon is currently under investigation in our laboratory and will be the subject of a subsequent report.

3.2. Continuous flow NO_x reduction over SCR catalyst

To investigate the ability of the Cu–zeolite SCR catalyst to utilize different reductants, steady state, continuous flow NO_x reduction experiments were conducted using ethene and propene Given that during engine-based LNT(-SCR) regeneration residual oxygen is typically present in the rich gas produced by the engine, the effect of oxygen concentration on NO_x reduction was also examined in these experiments. Results for propene are summarized in Fig. 5. As shown, the NO_x conversion was relatively low in the absence of O_2 but increased substantially when 1% O_2 was added to the feed, reaching a maximum of 80% (Fig. 5a). Further increase of the O_2 concentration resulted in decreased NO_x conversion. Similar results were obtained when 5000 ppm C_2H_4 was used as the reductant (data not shown), albeit that C_2H_4 was significantly less active in NO_x reduction than C_3H_6, a maximum NO_x conversion level of 64% being attained (at a feed O_2 content of 1%). These findings are similar to those reported by other researchers for Cu zeolite catalysts [29–31]. Iwamoto [30] reported that NO_x conversion by C_3H_6 over Cu-ZSM-5 reached a maximum in the presence of 1% O_2 (as opposed to 0% O_2 or ≥2% O_2). Petersson [31] reported that NO_x conversion by propene over Cu-FER + HZSM-5 attained its maximum value in the presence of 2% O_2. Evidently, there is an optimal concentration of O_2 in the $C_nH_{2n} + NO_x + O_2$ reaction, which appears to depend on the catalyst and presumably the ratio of C_nH_{2n} to NO_x. It should also be noted that the selectivity of NO_x reduction to N_2 was high in these experiments, being typically better than 95%.

It is generally accepted that the first step in the reduction of NO_x by hydrocarbons over Cu zeolite catalysts corresponds to NO oxidation (Eq. (3)) [32,33]. Although the exact mechanistic details of hydrocarbon SCR are still the subject of some debate [34], evidence has been reported suggesting that for zeolite-based catalysts a portion of the NO_2 undergoes reduction to NH_3 [33,35] (or possibly an amine [33]), most likely via the intermediacy of isocyanate species which in turn are formed from organo-nitrogen species such as RNO_2 or $RONO$ (Eq. (4)) [32]. The final step in this scheme involves the selective catalytic reduction of NH_3 with NO_x to produce N_2. (Eqs. (1) and (2)). Given that total oxidation of the hydrocarbon with O_2 (Eq. (5)) also occurs, the concentration of reductant available for formation of organo-nitrogen intermediates is effectively limited. Hence, NO_x reduction should be favored at relatively low O_2 concentrations, when there is insufficient O_2 present for complete hydrocarbon oxidation to occur.
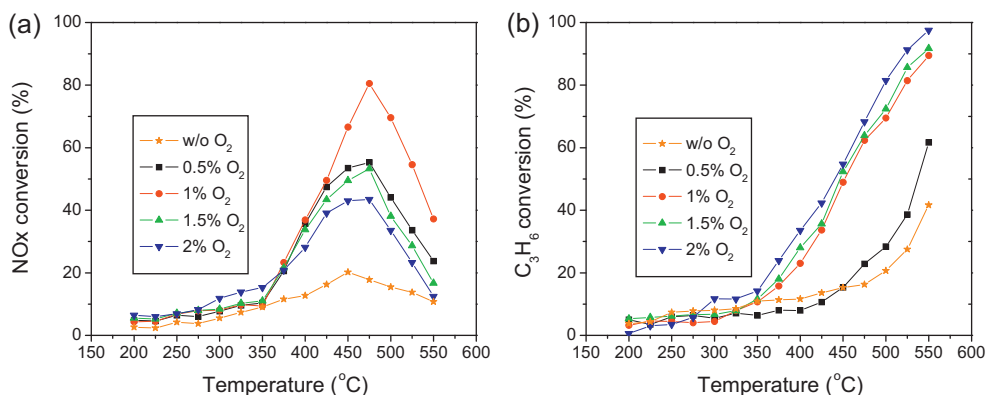
$$2NO + O_2 \rightarrow 2NO_2 \qquad (3)$$

$$NO_2 + C_xH_y \rightarrow R\text{-}NO_2 \text{ or } R\text{-}ONO \rightarrow -NCO \rightarrow NH_3 \qquad (4)$$

$$C_xH_y + (x + y/4)O_2 \rightarrow xCO_2 + y/2H_2O \qquad (5)$$

Fig. 5. NO$_x$ reduction with C$_3$H$_6$ over SCR catalyst under continuous flow conditions: (a) NO$_x$ conversion; (b) C$_3$H$_6$ conversion. Feed: 3333 ppm C$_3$H$_6$, 300 ppm NO, O$_2$ as indicated, 5% CO$_2$, 5% H$_2$O, N$_2$ as balance.

However, the reason why an O$_2$ concentration of 1% is optimal appears to be more subtle, since inspection of Fig. 5b reveals that there is little difference in propene conversion for experiments run with 1%, 1.5% and 2% propene, i.e., the concentration of propene available should be roughly the same at most temperatures. However, at a concentration of 1% O$_2$ (with 3333 ppm C$_3$H$_6$ present) the conditions are not yet net oxidizing, since complete consumption of the propene by O$_2$ would generate CO according to Eq. (6) (which in the absence of O$_2$ can also act as an efficient reductant):

$$C_3H_6 + 3O_2 \rightarrow 3CO + 3H_2O \qquad (6)$$

$$C_3H_6 + 4.5O_2 \rightarrow 3CO_2 + 3H_2O \qquad (7)$$

At higher O$_2$ concentrations there will be a tendency for CO$_2$ to be formed according to Eq. (7). Hence, the optimum O$_2$ concentration for NO$_x$ conversion is likely to be a function of the total number of reducing equivalents present, i.e., the hydrocarbon concentration and type.

3.3. NO$_x$ reduction over SCR catalyst under lean-rich cycling conditions

NO$_x$ reduction over the SCR catalyst was also studied under lean-rich cycling conditions. In order to mimic rich phase NO$_x$ slip from a LNT catalyst, in these experiments NO (300 ppm) was fed in both the rich and lean phases. Fig. 6a summarizes the cycle-averaged NO$_x$ conversions measured with 5000 ppm C$_2$H$_4$ and 3333 ppm C$_3$H$_6$ added in the rich phase, while the cycle-averaged hydrocarbon conversion is depicted in Fig. 6b. In each case, experiments

were run both without O$_2$ present in the rich phase, and with 1% O$_2$ present. In the case of NO$_x$ reduction with C$_3$H$_6$, NO$_x$ reduction was improved by the addition of 1% O$_2$, while a very slight improvement was similarly noted when C$_2$H$_4$ was used as the reductant. Again, these observations are consistent with the results of the continuous flow measurements, as is the finding that propene is a better reductant than ethene. However, in the case of NO$_x$ reduction with C$_3$H$_6$, a discrepancy was observed with respect to the catalyst inlet temperature at which the maximum NO$_x$ conversion of 27% was obtained, i.e., 350 °C under cycling, versus 475 °C for the continuous flow conditions. This can be explained by the fact that under cycling conditions a significant exotherm is generated across the catalyst due to the high propene feed concentration. Indeed, at the 350 °C inlet temperature, the catalyst outlet temperature typically varied between 400 °C and 425 °C (while mid-bed temperatures may have been even higher). It should also be noted that the selectivity of NO$_x$ reduction to N$_2$ in these experiments was high, the selectivity to N$_2$O not exceeding 1% at most temperatures.

Analysis of the NO$_x$ concentration profiles measured at the reactor outlet during these experiments is particularly informative. Fig. 7a and b show the C$_3$H$_6$, NO, NO$_2$ and NO$_x$ concentration profiles during cycling at 350 °C. The C$_3$H$_6$ signals correspond to the rich phases, the measured peak concentration of ca. 1800 ppm being significantly less than the feed concentration of 3333 ppm; hence, it is clear that significant propene conversion and/or storage occurs across the SCR catalyst. In comparison to the comparatively narrow C$_3$H$_6$ signals, the dips in NO$_x$ concentration are very broad. While the decrease in effluent NO$_x$ concentration clearly reaches a maximum in the rich phase, the NO$_x$ concentration returns to its
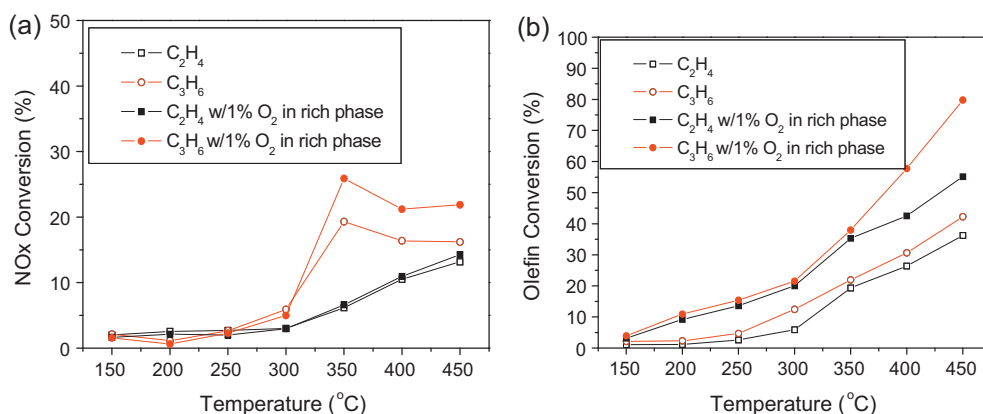

Fig. 6. NO$_x$ reduction over SCR catalyst during lean-rich cycling using 3333 ppm C$_3$H$_6$ and 5000 ppm C$_2$H$_4$ as rich phase reductants: (a) NO$_x$ conversion; (b) olefin conversion. Other gas components: lean (60 s): 300 ppm NO, 8% O$_2$, 5% CO$_2$, 5% H$_2$O, N$_2$ as balance; rich (5 s): 300 ppm NO, O$_2$ as indicated, 5% CO$_2$, 5% H$_2$O, N$_2$ as balance.
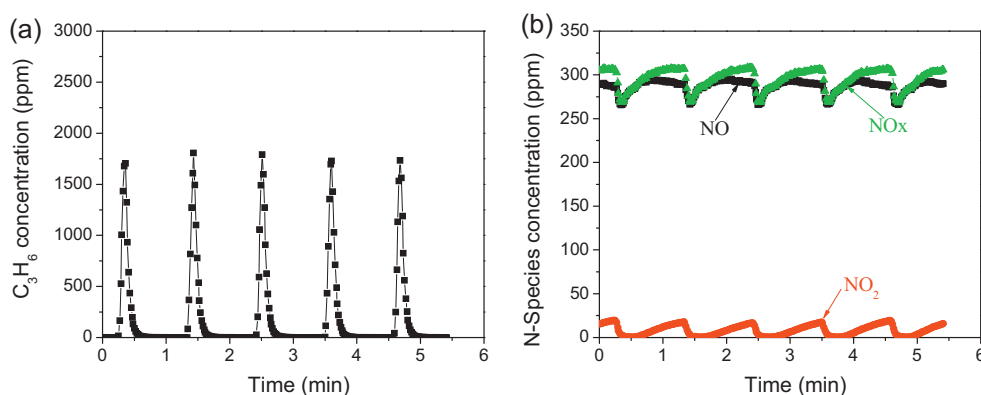
Fig. 7. (a) Measured propene concentration and (b) NO_x concentration in reactor effluent during lean-rich cycling over SCR catalyst at 350 °C. Feed: lean (60 s): 300 ppm NO, 8% O_2, 5% CO_2, 5% H_2O, N_2 as balance; rich (5 s): 300 ppm NO, 3333 ppm C_3H_6, 5% CO_2, 5% H_2O, N_2 as balance.

feed value only very slowly after the rich to lean transition is made; indeed, the feed NO_x concentration of 300 ppm is not attained until just before the subsequent lean to rich transition. This observation is consistent with the occurrence of NO_x conversion during the lean phase, indicating that the hydrocarbon is still available for NO_x reduction after its removal from the feed. This implies that propene is stored in the catalyst during the rich phase (albeit that some of the propene is consumed by rich phase NO_x reduction and that some of it slips through the catalyst), the stored propene being consumed during the subsequent lean phase.

Finally, it is worth noting that the form of the NO_2 profile indicates that during lean operation, a small amount of NO is oxidized over the catalyst to NO_2. During the rich phase NO oxidation drops to zero, while after the switch back to lean conditions the NO_2 concentration slowly climbs to its maximum value. This observation is also consistent with the consumption of stored hydrocarbon which inhibits the production of NO_2 during the initial part of the lean phase, potentially either via its reaction with NO_2 (as the latter forms) or via the inhibition of NO oxidation on the hydrocarbon-covered Cu sites.

3.4. Alkene and NH_3 adsorption experiments

In order to examine the degree to which hydrocarbons can be stored by the SCR catalyst, adsorption experiments were performed using C_3H_6 and, for comparison, NH_3. Fig. 8 depicts propene
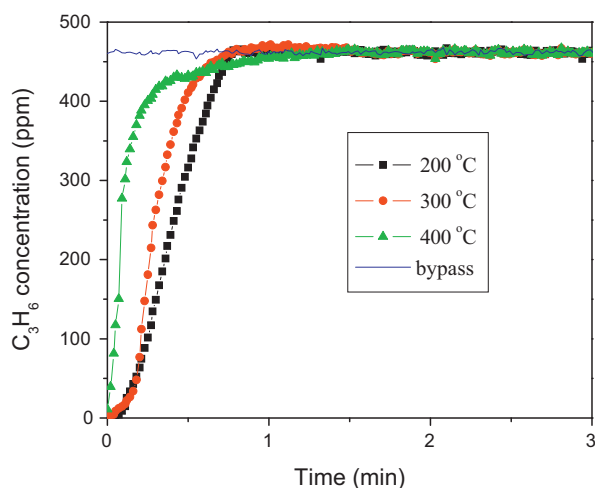

Fig. 8. Adsorption of C_3H_6 on SCR catalyst at different temperatures. Feed: 460 ppm C_3H_6, 5% CO_2, 5% H_2O, N_2 as balance.

Table 5
Measured adsorption capacity of SCR catalyst for NH_3 and C_3H_6.[a]

Adsorbate	Adsorption capacity (μmol/g)		
	200 °C	300 °C	400 °C
C_3H_6	72	69	30
C_3H_6 (w/NH_3 present)	42	39	16
NH_3	541	313	172
NH_3 (w/C_3H_6 present)	557	338	173

[a] Feed: 460 ppm C_3H_6 (when present), 500 ppm NH_3 (when present), 5% CO_2, 5% H_2O, N_2 as balance.

uptake curves at 200 °C, 300 °C and 400 °C, while Table 5 collects the measured adsorption capacities for propene and NH_3. These results show that the catalyst possesses significant adsorption capacity for both NH_3 and propene. Unsurprisingly, the adsorption capacity for NH_3 is significantly greater than that for the bulkier and less Lewis basic C_3H_6, while the adsorption capacity for both species decreases with increasing temperature. Co-adsorption experiments were also performed, employing a feed containing an equal concentration of propene and NH_3. As shown in Table 5, the presence of C_3H_6 does not greatly affect the adsorption capacity for NH_3, although a slight increase in NH_3 adsorption is observed at 200 °C and 300 °C in the presence of C_3H_6. This was consistently observed in replicate experiments, although the reasons for it are not entirely clear. In contrast, C_3H_6 adsorption is decreased in the presence of NH_3, although significant adsorption still occurs. This finding suggests that to some extent NH_3 and C_3H_6 adsorb at different sites on the catalyst. According to Efremov and Davydov [36], C_3H_6 adsorbs on CuO/Al_2O_3 and Cu(II)YA zeolite via the formation of stable π-complexes with Cu(I). The Cu(I) is formed via electron exchange between the C=C bond and Cu(II) with the formation of carbocations. Parrillo et al. [37] observed strong propene uptake in Cu-ZSM-5 and concluded that propene interacts strongly with Cu that is present at the Al sites in a stoichiometry close to 1/Cu at room temperature. Also of relevance in this context is a study by Li et al. [38] concerning the mechanism of propene poisoning of Fe-ZSM-5 in NO_x reduction by NH_3. These workers found that in the presence of propene NO adsorption on Fe^{3+} sites was blocked by (propene-derived) carbonaceous deposits. In contrast, NH_3 adsorption, which occurred on Brønsted acid sites, was not significantly affected by the presence of propene.

In the case of NH_3, adsorption in Cu–zeolites can in principle occur at Brønsted acid sites (as for Fe-ZSM-5) and at Cu ions. Brønsted acid sites are typically associated with residual protons which are not removed during introduction of the metal ion in the zeolite. For Cu-ZSM-5, Brønsted acid sites have also been observed which correspond to defective Al(III) sites in the zeolite [39], as have
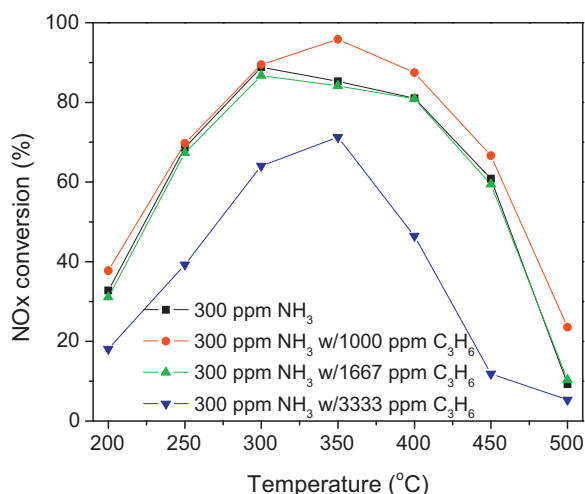
Fig. 9. Effect of C_3H_6 addition on $NO + NH_3$ reaction over SCR catalyst under continuous flow conditions. Feed: 300 ppm NO, 300 ppm NH_3, C_3H_6 as indicated, 8% O_2, 5% CO_2, 5% H_2O, N_2 as balance.

Fig. 10. Cycle-averaged NO_x conversion over SCR catalyst using NH_3, C_3H_6 and $NH_3 + C_3H_6$ as reductants. NH_3 and C_3H_6 concentrations as indicated; other feed conditions as for Fig. 7. The dotted line is included as a guide and represents the sum of the NO_x conversions obtained in the separate experiments using 300 ppm NH_3 and 3333 ppm C_3H_6.

protonic sites introduced into the zeolite during the exchange process with Cu ions [37]. Additionally, if propene adsorption results in the formation of carbocations, then NH_3 adsorption should occur with proton abstraction to generate NH_4^+ and carbon-based radical species. Conceivably, this might explain the slight increase in NH_3 adsorption observed during NH_3/C_3H_6 co-adsorption experiments. Evidence is also available for the adsorption of NH_3 on Cu sites. Several workers have reported the formation of stable Cu ammine complexes as the result of NH_3 adsorption on Cu(II)-Y zeolite [40,41]. Similarly, a more recent study [39] of NH_3 adsorption on Cu-ZSM-5 found that a $[Cu(NH_3)_4]^+$ complex was formed at room temperature (based on volumetric adsorption and IR spectroscopic data).

The finding that significant co-adsorption of NH_3 and propene can occur implies that at these moderate concentrations (~500 ppm of each adsorbate), NO_x reduction by NH_3 and by C_3H_6 can proceed in parallel. In order to test this idea, continuous flow and lean-rich cycling experiments were performed comparing NO_x reduction efficiency using NH_3, C_3H_6 and a $NH_3 + C_3H_6$ mixture as the reductants. The results of these experiments are summarized in Figs. 9 and 10. As shown in Fig. 9, under continuous flow (lean) conditions, the addition of 1000 ppm C_3H_6 to a feed containing 300 ppm NO and 300 ppm NH_3 resulted in a modest improvement in the NO_x conversion in the temperature range of 350–500 °C. This range corresponds to the window for which NO_x reduction with C_3H_6 is close to, or at, its maximum under cycling conditions (see Fig. 6a). This indicates that the effects of NH_3 and C_3H_6 on NO_x reduction are to a large degree additive under these conditions. However, increase of the feed C_3H_6 concentration to 1667 ppm caused a decrease in NO_x reduction activity in the 350–500 °C range, such that NO_x conversions were similar to those measured in the absence of C_3H_6. Further increase of the feed C_3H_6 concentration to 3333 ppm resulted in NO_x conversion levels which were substantially lower than those obtained with NH_3 alone, indicating that high C_3H_6 concentrations inhibit NO_x reduction by NH_3. Interestingly, this inhibition is not observed under cycling conditions (Fig. 10). As shown, the cycle-averaged NO_x conversion obtained when 3333 ppm of C_3H_6 and 300 ppm of NH_3 are added in the rich phase correlates fairly well with the sum of the conversions obtained with NH_3 and C_3H_6 separately (denoted in Fig. 10 by the dotted line). The observed difference between continuous flow and cycling results can be attributed to the fact that under cycling conditions the reductant is added for only a small portion of the cycle
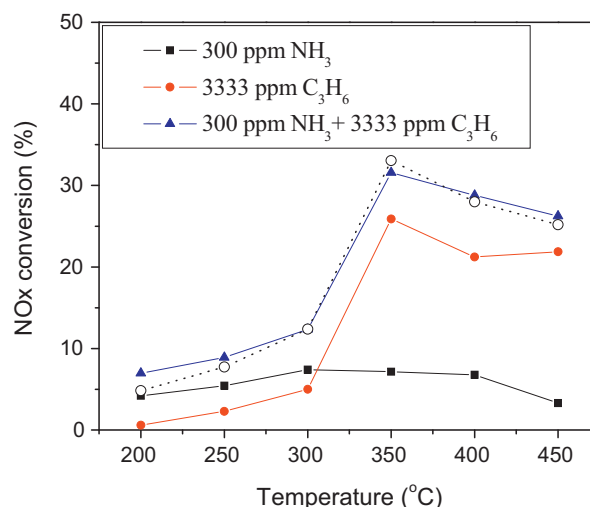
(one-thirteenth of the total cycle time). Hence, NO_x conversion should be reductant-limited for most of the cycle. This contrasts with the continuous flow conditions, in which 3333 ppm C_3H_6 is continuously supplied to the catalyst, which can be expected to result in some degree of blocking of the active sites by C_3H_6, this being a less active reductant than NH_3.

The finding that NO_x reduction by NH_3 and by C_3H_6 can proceed in parallel during cycling is significant because it suggests that under actual driving conditions, NO_x reduction by hydrocarbons in the SCR catalyst will contribute to the mitigation of NO_x emitted by the LNT catalyst during rich phase regeneration (the so-called NO_x puff), as well as NO_x that may slip through the LNT catalyst during the initial part of the lean phase (albeit that the latter should be minimal). That said, it should be appreciated that the contribution to NO_x reduction by non-NH_3 reductants will be highly dependent on the nature of the catalysts employed in the LNT-SCR system. Specifically, we have observed that these effects are most significant when a low precious metal-loaded LNT is used, in combination with the commercial Cu–zeolite SCR catalyst employed in this study. LNT catalysts possessing high Pt and Rh loadings tend to be highly efficient, such that NO_x conversion is mainly confined to the LNT catalyst, the role of the SCR catalyst being confined to eliminating NH_3 and NO_x slip at low temperatures. In addition, Fe-zeolite catalysts are not as effective in enhancing LNT performance as the Cu–zeolite SCR catalyst used in this study [14].

Finally, it is worth noting that the ability of the SCR catalyst to trap hydrocarbons (HCs) not only offers the prospect of HC-SCR of NO_x, it also provides advantages for HC emission control over the LNT-only system. By trapping HC slip from the LNT during rich purges and storing it until it can be oxidized during subsequent lean operation, total HC emissions can be decreased. Indeed, a recent demonstration involving vehicle and laboratory tests has provided strong evidence for this additional benefit [42].

4. Conclusions

Coupled LNT-SCR systems represent a promising approach for the mitigation of NO_x emissions from lean-burn engines. In this study it was found that in addition to the NH_3 pathway for NO_x conversion, a second pathway can operate in the SCR catalyst of LNT-SCR systems which is associated with the presence

of hydrocarbons. LNT-SCR lean-rich cycling experiments revealed that when a $CO + H_2 + C_3H_6$ mixture or C_3H_6 by itself was used as the reductant, more NO_x was converted over the SCR catalyst than could be accounted for by NH_3 emitted from the LNT catalyst. This finding is attributed to the reaction of propene, which slipped through the LNT catalyst, with NO_x slip from the LNT. Separate experiments, conducted under continuous flow and lean-rich cycling conditions, have confirmed the ability of propene and ethene to function as NO_x reductants over the SCR catalyst. The cycling experiments also show that the SCR catalyst is able to store propene, such that NO_x reduction by stored propene can continue into the lean phase (after the switch from rich conditions). According to the results of adsorption experiments, significant co-adsorption of NH_3 and propene can occur in the SCR catalyst, while under lean-rich cycling conditions the contributions of NH_3 and C_3H_6 to NO_x conversion are found to be essentially additive. This finding suggests that under actual driving conditions, NO_x reduction by non-NH_3 reductants (olefins and possibly other hydrocarbons) in the SCR catalyst can contribute to the mitigation of NO_x emitted by the LNT catalyst during rich phase regeneration, in addition to NO_x that slips through the LNT catalyst during the initial part of the lean phase.

Disclaimer

This report was prepared as an account of work sponsored by an agency of the United States Government. Neither the United States Government nor any agency thereof, nor any of their employees, makes any warranty, express or implied, or assumes any legal liability or responsibility for the accuracy, completeness, or usefulness of any information, apparatus, product, or process disclosed, or represents that its use would not infringe privately owned rights. References herein to any specific commercial product, process, or service by trade name, trademark, manufacturer, or otherwise does not necessarily constitute or imply its endorsement, recommendation, or favoring by the United States Government or any agency thereof. The views and opinions of authors expressed herein do not necessarily state or reflect those of the United States Government or any agency thereof.

Acknowledgements

References

[1] H. Hu, J. Reuter, J. Yan, and J. McCarthy, Jr., SAE Technical Paper 2006-01-3552, (2006).
[2] K.E. Bevan, W. Taylor, III, SAE Technical Paper 2006-01-3551, (2006).
[3] R. Roecker, R. Zhan, R.H. Stanglmaier, SAE Technical Paper 2007-01-3983, (2007).
[4] R. Snow, G. Cavataio, D. Dobson, C. Montreuil, R. Hammerle, SAE Technical Paper 2007-01-1244, (2007).
[5] R. Snow, D. Dobson, R. Hammerle, S. Katare, SAE Technical Paper 2007-01-0469, (2007).
[6] T. Nakatsuji, M. Matsubara, J. Rouistenmäki, N. Sato, H. Ohno, Appl. Catal. B 77 (2007) 190.
[7] H. Shinjoh, N. Takahashi, K. Yokota, Top. Catal. 42–43 (2007) 215.
[8] X. Chen, J. Schwank, Top. Catal. 46 (2007) 39.
[9] E.C. Dykes, SAE Technical Paper 2008-01-2642, (2008).
[10] E.C. Corbos, M. Haneda, X. Courtois, P. Marecot, D. Duprez, H. Hamada, Appl. Catal. A 365 (2009) 187.
[11] L. Xu, R. McCabe, W. Ruona, G. Cavataio, SAE Technical Paper 2009-01-0285, (2009).
[12] M. Weibel, N. Waldbüsser, R. Wunsch, D. Chatterjee, B. Bandl-Konrad, B. Krutzsch, Top. Catal. 52 (2009) 1702.
[13] R. Zukerman, L. Vradman, M. Herskowitz, E. Liverts, M. Liverts, A. Massner, M. Weibel, J.F. Brilhac, P.G. Blakeman, L.J. Peace, Chem. Eng. J. 155 (2009) 419.
[14] L. Xu, R. McCabe, M. Dearth, W. Ruona, SAE Technical Paper 2010-01-0305, (2010).
[15] D. Chatterjee, P. Kočí, V. Schmeisser, M. Marek, M. Weibel, B. Krutzsch, Catal. Today 151 (2010) 395.
[16] R. Bonzi, L. Lietti, L. Castoldi, P. Forzatti, Catal. Today 151 (2010) 376.
[17] P. Forzatti, L. Lietti, Catal. Today 155 (2010) 131.
[18] A. Lindholm, H. Sjövall, L. Olsson, Appl. Catal. B 98 (2010) 112.
[19] J. Wang, Y. Ji, V. Easterling, M. Crocker, M. Dearth, R.W. McCabe, Catal. Today 175 (2011) 83.
[20] J.A. Pihl, J.E. Parks II, C.S. Daw, T.W. Root, SAE Technical Paper 2006-01-3441, (2006).
[21] F. Plát, S. Bártová, J. Štěphánek, P. Kočí, M. Marek, Ind. Chem. Eng. Res. 49 (2010) 10348.
[22] C.-K. Seo, H. Kim, B. Choi, M.T. Lim, C.-H. Lee, C.-B. Lee, Catal. Today 164 (2011) 507.
[23] Unpublished data, Ford Motor Co.
[24] J.H. Kwak, R.G. Tonkyn, D.H. Kim, J. Szanyi, C.H.F. Peden, J. Catal. 275 (2010) 187.
[25] L. Gang, J. van Grondelle, B.G. Anderson, R.A. van Santen, J. Catal. 186 (1999) 100.
[26] P. Joza, E. Jobson, M. Larsson, Top. Catal. 30/31 (2004) 177.
[27] S. Poulston, R. Rajaram, Catal. Today 81 (2003) 603.
[28] A.A. Phatak, N. Koryabkina, S. Rai, J.L. Ratts, W. Ruettinger, R.J. Farrauto, G.E. Blau, W.N. Delgass, F.H. Ribeiro, Catal. Today 123 (2007) 224.
[29] M. Iwamoto, N. Mizuno, H. Yahiro, Stud. Surf. Sci. Catal. 75 (1993) 1285.
[30] M. Iwamoto, H. Yahiro, S. Shundo, Y. Yu-u, N. Mizuno, Appl. Catal. 69 (1991) L15.
[31] M. Petersson, T. Holma, B. Andersson, E. Jobson, A. Palmqvist, J. Catal. 235 (2005) 114.
[32] N.W. Cant, I.O.Y. Liu, Catal. Today 63 (2000) 133.
[33] H.-Y. Chen, Q. Sun, B. Wen, Y.-H. Yeom, E. Weitz, W.M.H. Sachtler, Catal. Today 96 (2004) 1.
[34] O. Gorce, F. Baudin, C. Thomas, P. Da Costa, G. Djega-Mariadassou, Appl. Catal. B 54 (2004) 69.
[35] F. Poignant, J. Saussey, J.C. Lavalley, G. Mabilon, J. Chem. Soc.: Chem. Commun. (1995) 89.
[36] A.A. Efremov, A.A. Davydov, Kinet. Kataliz. 24 (1983) 1180.
[37] D.J. Parrillo, D. Dolenec, R.J. Gorte, R.W. McCabe, J. Catal. 142 (1993) 708.
[38] J. Li, R. Zhu, Y. Cheng, C.K. Lambert, R.T. Yang, Environ. Sci. Technol. 44 (2010) 1799.
[39] V. Bolis, S. Maggiorini, L. Meda, F. D'Acapito, G. Turnes Palomino, S. Bordiga, C. Lamberti, J. Chem. Phys. 113 (2000) 9248.
[40] E.F. Vansant, J.H. Lunsford, J. Phys. Chem. 76 (1972) 2860.
[41] Y.-Y. Huang, J. Catal. 30 (1973) 187.
[42] L. Xu, R. McCabe, P. Tennison, H.-W. Jen, SAE Technical Paper, 2011-01-0308.